# Collocated Ground Deformation and Pore Pressure Measurements in Open Pit Mines: Laboratory Testing and Analysis of Wireless Sensing Platform


**E. Widzyk-Capehart, A. Barberán, M. J. Briceño, C. Navarro, P. M. V. Nguyen, C. Opazo and S. Steffen**

## 1 Introduction

In the design of open pit mines, the geomechanical properties of the rock mass are one of the critical sources of uncertainty, which affect the stability of slopes with results that can be catastrophic: the design can drastically influence mining production and its economic viability [1]. Therefore, there are multiple challenges when assessing subsurface deformations and variation in pore pressure within the rock mass mainly because there are a limited number of devices that can be installed inside the boreholes. In addition, the correlation of displacement data with pore pressure, especially in low-permeability environments, is complex the respective sensors are installed in separate drill holes.

Rigorous monitoring of surface and subsurface to determine the displacement is one of the ways to have a general assessment of the behavior of the slopes, allowing for the protection of personnel and equipment, maintaining safer operating conditions; early notifications of potentially unstable areas; provision of geotechnical information to analyze any slope instability mechanism that may be developed, allowing the development of appropriate corrective action plans leading to the improvement of future slope design as well as evaluating the performance of the slope design implemented.

E. Widzyk-Capehart · P. M. V. Nguyen
Advanced Mining Technology Center (AMTC), University of Chile, Santiago, Chile

A. Barberán · C. Navarro (✉) · C. Opazo
CSIRO Chile International Centre of Excellence, Santiago, Chile
e-mail: canavarr.ing@gmail.com

M. J. Briceño
Independent Consultant, Santiago, Chile

S. Steffen
Elexon Electronics, Brendale, Australia



E. Widzyk-Capehart et al. (eds.), *Proceedings of the 27th International Symposium on Mine Planning and Equipment Selection - MPES 2018*,
https://doi.org/10.1007/978-3-319-99220-4_31

The surface slope displacement monitoring instruments are quite sophisticated with automatic wireline extensometers, universal EDM stations, 3D digital photogrammetry and laser scanning and ground-based and satellite-based radars. All of them can provide us with a real-time 3D record of any surface movement that may occur around the walls of the pit [2]. However, in-ground movement monitoring instruments are less sophisticated. Typically, they include shear strips and/or time domain reflectometers (TDR), extensometers, and inclinometers placed in boreholes to locate the propagation of subsurface movement after evidence of subsurface deformation has been detected [3]. Less typically, they are placed where it is expected that the surface instruments cannot detect movement, sometimes being able to detect deformation in real time as it propagates to the surface. Most of the time, subsurface sensors are adapted from civil engineering applications to mining; often they do not work well in some areas because the deformation to which they are subjected, affects their casing, restricting the internal movement of the sensor or even causing breakage of communication cables, as is the case with inclinometers and Shape Accelerometer Array (SAA) [4].

To address the disadvantages of today's ground instrumentation, the use of wireless sensor technology with multiple detection capabilities, providing more robust system without dependence on cable connection for the transmission of data to the surface, possibility to combine measurements of different variables within a single unit, capability to install an array of sensors in a single hole, ease of installation.

In this article, the latest developments of the monitoring platform that combines the measurement of deformations and pore pressure with the wireless transmission of data in real time are described.

## 2 Enhanced Networked Smart Markers (ENSM)

The Enhanced Networked Smart Markers (ENSM) are electronic devices developed by Elexon Electronics, which represent the evolution of their previous technology, the Smart Markers (SM). The current ENSMs (Fig. 1) are equipped with an accelerometer and a magnetometer, to measure the inclination (ENSM Tilt) or, additionally, with a piezometer (ENSM Pore-pressure). The device includes radio transceivers (Green) that operate on battery, incorporating a plastic housing (Yellow) of 34.5 cm long and 6.35 cm in diameter, filled with epoxy material, and protections (White and blue) for radio transceivers and battery to improve the resistance of the product to blasting [5–7].

### *2.1 Deformation Measurements*

The main deformation measuring device in open pit mines is an inclinometer, which measures the rock movement with respect to the vertical axis through a gravity

**Fig. 1** Prototype of new ENSM adapted to the NSM case [8]

sensing transducer [9, 10]. Deformation measurement within the ENSM platform is accomplished using a three-axis MEMS accelerometer and magnetometer. The magnetometer provides three orthogonal channels of magnetic field measurement, while each of the channels provides an orientation to the movement detected by the accelerometer. The data obtained from the three axes accelerometer readings allow to determine horizontal and vertical displacements in the position of the marker.

## *2.2 Pore Pressure*

Reductions in groundwater pressure increase the effective tension in the rock mass and, as a consequence, increase the shear strength. In some cases, the dehydration of the rock mass is the only way to increase its resistance, therefore reducing the probability of slope failure [11]. The precise characterization of the vertical distribution of pore pressure requires in situ pressure measurements at different depths and is particularly important if vertical gradients are relevant, such as in open pit mines and in operations with active depressurization programs.

At present, geotechnical engineering uses several types of piezometers to measure pore pressure, among which, stand out the vibrating rope piezometers, which predominate in open pit mines, which are installed in boreholes that are filled with grouting and bentonite by the total injection method, process that undergoes these sensors, during this process of "grouting" (and before setting) to load pressures can increase depending on the depth of the well and the density of the grout; The head pressure (pressure head) exerted by the grout is higher than the pressure of the head of an equivalent water column, mainly due to the density of the grout, therefore, the sensor must withstand a wide range of pressures while maintaining the accuracy of the measurement after installation [12].

The pore pressure measurement within the ENSM is accomplished using the TTF-1 pressure transducer, manufactured by the German company Wika [13], which has been selected for its precision and ability to withstand overpressures. This sensor

must be protected against blockage and mechanical damage while allowing the flow of water. Therefore, a 48 μm steel mesh has been installed, which allows the passage of water but not of the slurry, providing protection to the sensor without the water pressure measurements being altered. The initial results of the laboratory testing of the pore pressure sensor were reported in [8, 12].

## 3 ENSM Testing and Results

A series of tests were carried out at the Elexon's laboratories in Brisbane, Australia and at the Advanced Center for Mining Technology (AMTC) of the University of Chile in Santiago de Chile.

### *3.1 Inclinometer Testing*

Three different test configurations (angles) were carried out in the laboratory to analyze the accuracy of the inclinometers. The antenna remained fixed at one end, at the other end was the marker raised to different heights with respect to the fixed point (0, 15 and 30 cm). For each position, the readings of the accelerometer (*Ax*, *Ay*, *Az*) and the magnetometer (*Bx*, *By*, *Bz*) were recorded. Figure 2 shows the accelerometer readings and Fig. 3 shows the magnetometer readings on the three axes. The first position (0 cm) is shown in first 7 samples (1–7), the second position (15 cm) in 3 samples (8–10), and third position (30 cm) in 30 samples (11–30).

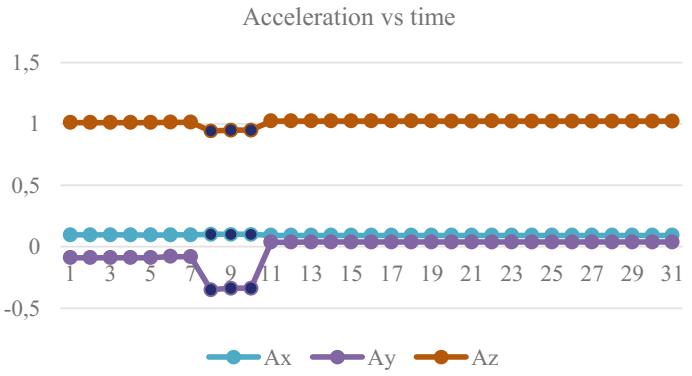


**Fig. 2** Accelerometer readings (linear gravity vector) over time (iteration)

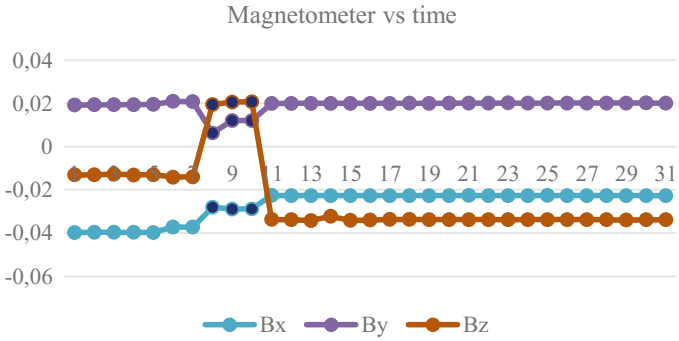


**Fig. 3** Magnetometer readings (gauss magnetic vector) over time (iteration)

## *3.2 Tilt Sensor Testing*

The test set-up involved a small slab of granite rock (stone kitchen bench material), with 14 ENSM devices glued to it. The rock was suspended on springs in an insulated and thermally regulated chamber specifically made for this test. The thermal chamber kept the devices at a constant 36° ± 0.5° temperature.

With MEMs devices, the accelerometer readings vary with temperature. However, the temperature in the ground deeper than a few meters tends to be quite constant at approx. ±0.5° difference, which will thus ensure stability of the readings at greater depths.

Each data point in Figs. 4 and 5 represents a reading taken from an ENSM device. The sensor dataset recorded by each device consists of three-axis acceleration readings, three-axis magnetometer reading, and temperature. The three-axis accelerometer readings were combined into the devices' roll and pitch values. Figures 4 and 5 show that the sensors are recording highly correlated changes in tilt direction and extent. This recorded movement is due to the floor of the building's tilt-slab concrete deforming. There are variations between various devices readings. Some of the variations are attributed to the effect that changing temperature has on the accelerometer. Some of it can be interpreted as noise. The error in the readings is approximately a quarter of the amount that concrete laboratory floor is moving. The error is ±0.05° which translates into approx. 2.5 mm over a 3 m length (or submillimeter over 1 m). The resolution of the sensor is about 1 mm over a 3 m length (Fig. 4). The temperature in the chamber is being varied by ±0.5 °C (Fig. 5). The analysis of the data suggests that approximately 50% of the errors are caused by the variation in temperature. At this stage, the error is constant over time; the readings are not diverging as time goes on.

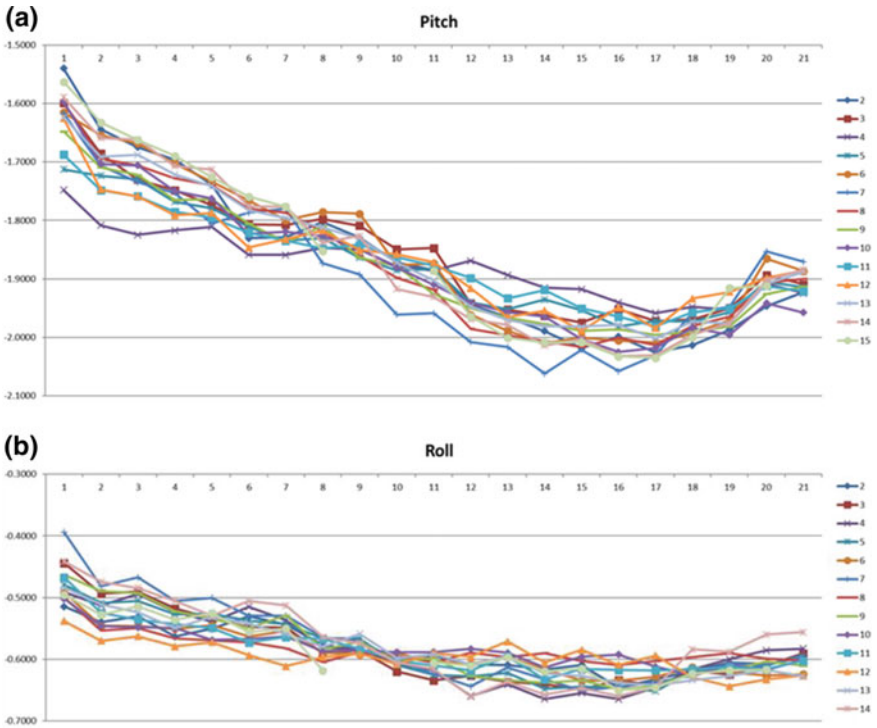


**Fig. 4** Pitch (**a**) and roll (**b**) values (angles) versus time (days)

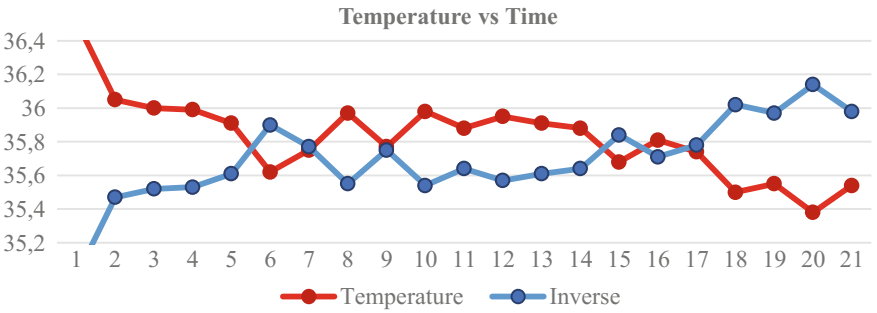


**Fig. 5** Temperature in the test chamber (Celsius) versus time (days)

## *3.3 Pore Pressure Measurement*

One of the key factors that could affect the correct measurements of pore pressure is the permeability of the grout and the time lag until the sensor is exposed to the water pressure present in the rock. The grout permeability can be up to two or three orders of magnitude greater than the permeability of the rock, which reaches

$10^{-6}$ to $10^{-8}$ cm/s. This range is controlled by the water/cement ratio. The time lag depends on the type of sensor, the volume of water required to record the variation of the recorded pressures, the grout permeability, the formation of air bubbles during installation and the degree of the grout saturation.

### 3.3.1 Grouting Properties

For the installation of the ENSM in the borehole, grouting mixture is used to fix the sensors in place. In Chile, pozzolanic cement instead of Portland cement is generally used to create the grout [14, 15]. Therefore, tests were carried out to examine the possible differences between the grouts with different cements; Pozzolanic cement and SuperGel-X CETCO. In addition, calcium bentonite or sodium bentonite can be used as sodium bentonite absorbs more water than calcium bentonite [15].

The result of the test to determine the influence of the type of bentonite on the grout behavior showed both types of grout behaved similarly during the setting and curing process, despite the differences in viscosity observed during processing, confirming that the type of bentonite does not influence the behavior of the grout [8].

### 3.3.2 Permeability and Saturation

The permeability and saturation test was carried out to determine the permeability and saturation degree of the bentonite cement grout, which is to be used in the field installation of the ENSM markers. In addition, possible variation in the curing time of the mixture and whether the permeability was within the parameters reported by [14] and [15] was also tested. The hypothesis was formulated that the use of pozzolanic cement could lead to a decrease in permeability as compared to Portland cement used internationally.

A flexible wall permeameter was used in triaxial equipment, at variable load, to measure the permeability ($K$) [16]. Three samples of grout were prepared and analyzed, the first at 7 days of curing, the second at 14 days and the third at 28 days (Fig. 6a).

All samples were tested at an effective pressure of 10 kPa. The corresponding sample at 14 days was also tested at 32.98 and 163 kPa effective chamber pressure of the permeameter (Fig. 6b). To allow the free flow of the grout during the field tests, the grout component proportions used were “water: cement: bentonite” in relation “2.5: 1: 0.25” (modified after [14]).

The degree of saturation is calculated according to Eq. 1:

$$S = V_w / V_v \tag{1}$$

where: $V_w$: volume of water and $V_v$ is the volume of voids; $V_v$: was obtained indirectly from the specific gravity of the particles (Eq. 2)

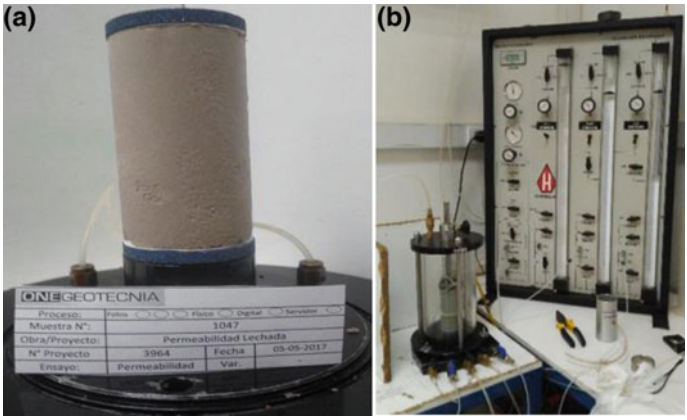


**Fig. 6** Grouting sample: **a** at 14 days of curing; **b** in a flexible wall permeameter

$$G_s = \gamma_s / \gamma_w \tag{2}$$

where: $\gamma_s$: volume of solids and $\gamma_w$: volume of water.

The unit weight of the sample was calculated as (Eq. 3):

$$\gamma = W_s / V_s \tag{3}$$

where: $W_s$: weight of solids and $V_s$: volume of solids.

The natural moisture of the sample was calculated as (Eq. 4):

$$\omega = W_w / W_s \tag{4}$$

where: $W_w$: weight of water and $W_s$: weight of solids.

The tests were performed according to the Chilean Standards [17, 18]. The permeability values obtained are shown in Table 1.

Figure 7 shows the results of permeability tests over time (7, 14 and 28 days with pressure of effective chamber of 10 kPa) and pressure (10, 32, 98 and 163 kPa). The permeability values are of the order of magnitude of 10–6 to 10–8 cm/s. The results show that the permeability increases by two orders of magnitude from 7 to 14 days of curing time. However, from 14 to 28 days of curing, the permeability is maintained within $10^{-6}$ m/s. The results show an expected increase in permeability

**Table 1** Results of permeability

| Sample (days) | Permeability (cm/s) |
|---|---|
| 7 | $6 \times 10^{-8}$ |
| 14 | $2 \times 10^{-6}$ |
| 28 | $5 \times 10^{-6}$ |

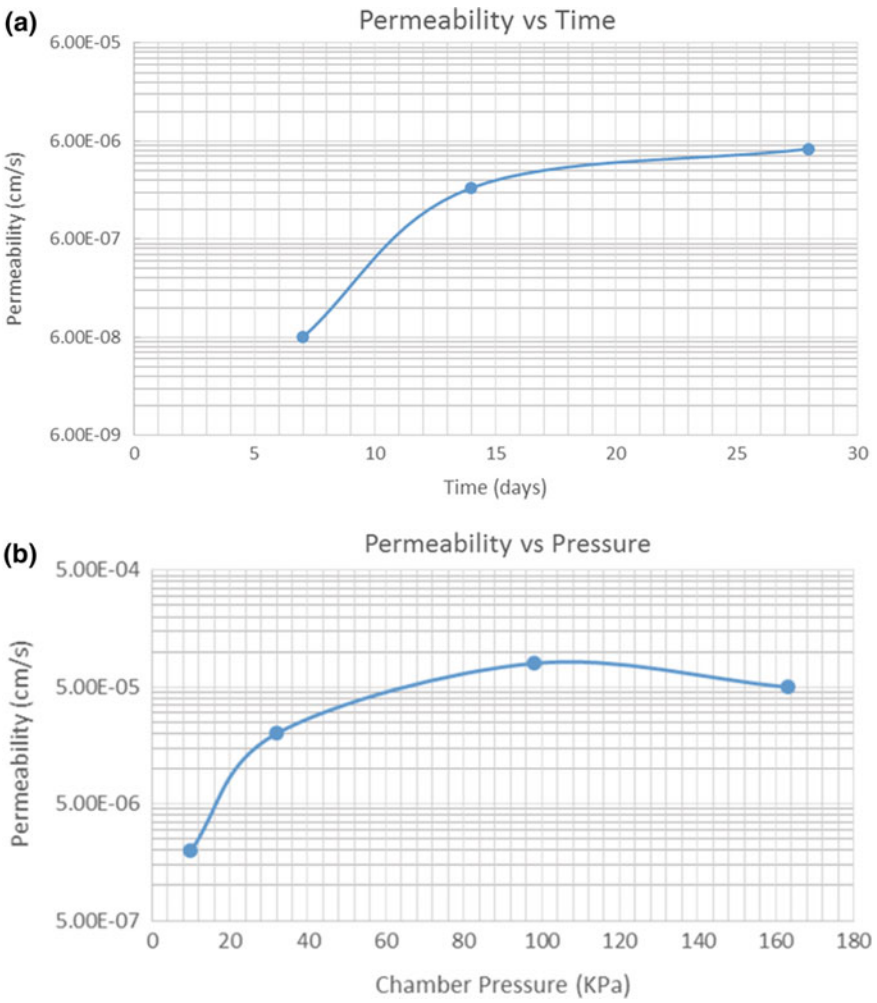


**Fig. 7** Permeability of the grout: **a** over time; **b** over chamber pressure

up to 14 days of curing; however, the expected linear behavior is not observable from day 14 onwards (Fig. 7a).

The effect of increase in pressure also shows a different behavior as the permeability increases with the pressure increase of 10–32 kPa. However, when reaching pressures in the range of 98–163 kPa, the permeability decreases (Fig. 7b).

Therefore, although the observed permeability values are within the order of magnitude, the influence of the pressure increase on the permeability does not match the results presented by [17] in the full pressure scale. As the tests were performed in accordance with Chilean standards, the results are unexpected in the highest range

of pressures and more investigations are being carried out to determine the source of this discrepancy.

## 4 Conclusions

The results of the tests carried out for the grout showed that the type of bentonite does not influence the curing process of the grout. However, the results of the permeability tests showed mixed results; while the permeability values were within the order of magnitude, the evolution of the permeability with respect to the curing time of the slurry and the pressure to which it was subjected, showed differences with the expected results as described in the literature.

The tilt sensor tests show that the error seems to be reasonably constant over time; the readings continue to ensure consistency in the results as time goes on, while simulating the field conditions in the laboratory and improvements are made to the processing algorithms to ensure the acquisition and processing of data in real time during testing of field. Finally, the sensors were calibrated to consider the variable of temperature change in the environment.

Additional tests are being carried out to analyze the response times of the pore pressure sensors based on the analysis of the grout test results of the new detection platform to determine: (1) the time elapsed between the installations of the sensors until the hydrostatic pressure of the medium begins to be measured. It is assumed that the duration of these tests is conditioned by the behavior of the slurry and is expected to be at least 28 days and (2) the response time after stabilization, that is, the time between a pressure disturbance in the mean and time that the sensor records the disturbance. This time depends on the volume of the water to be moved from the medium to the measuring chamber and the ease of the associated water to flow. Low response times are expected from minutes to hours.

**Acknowledgements** We would like to acknowledge the support of the following institutions: Conicyt through the FB0809 PIA CONICYT Grant and the Fundación CSIRO Chile through the Smart Open Pit Slope Management Project under the auspices of CORFO (INNOVA CORFO 10CEII-9007); the University of Chile, Advanced Mining Technology Center (AMTC), Elexon Electronics for their continuous collaboration in the development of this novel technology and Dr. John Read for his contribution at the inception of this technology and the project.

## References

1. Wyllie, D.C., Mah, C.W.: Movement monitoring. In: Wyllie, D.C., Mah, C.W. (eds.) Rock Slope Engineering, 4th edn. Spon Press, New York (2004)
2. Cook, D.: Robotic total stations and remote data capture: challenges in construction. Geotech. News **24**(3), 42–45 (2006)
3. Bayoumi, A.: On the evaluation of settlement measurements using borehole extensometers. Geotech. Geol. Eng. **29**(1), 75–90 (2011)

4. Dowding, C.H., O'Connor, K.M.: Comparison of TDR and inclinometers for slope monitoring. ASCE Geotech. Spec. Tech. Publ. **106**, 80–90 (2000)
5. Elexon Mining.: Networked Smart Marker System. Available at: http://www.elexonmining.com/networked-smart-markers-2. Accessed 1 Nov 2015
6. Whiteman, D.S.: The smart marker system—a new tool for measuring underground ore body flow in block and sub-level mines. In: 2nd International Symposium on Block and Sublevel Caving, pp. 603–622, Perth, Australia (2010)
7. Widzyk-Capehart, E., Hölck, C., Fredes, O., Pedemonte, I., Steffen, S.: Implementation of Novel Subsurface Deformation Sensing Device for Open Pit Slope Stability Monitoring—The Networked Smart Markers System, MPES 2015 (2015)
8. Widzyk-Capehart, E., Gonzalez, N., Pedemonte, I., Sanchez, E., Steffen, S.: Towards real-time, wireless in-ground simultaneous monitoring of rock deformation and pore pressure in open pit mines. MPES **2017**, 7 (2017)
9. Widzyk-Capehart, E., Hölck, C., Fredes, O., Sánchez, E., Pedemonte, I., Marciniak, M., Floría, E., Poulson, J., Steffen, S.: Emerging developments of the Networked Smart Markers System Towards an Integrated Monitoring Platform. Minin (2016)
10. Holck, C.: Open pit geomechanics and mine planning integration: design and economic assessment of a subsurface slope deformation monitoring campaign. M.Sc. Thesis, University of Chile (2016)
11. Beale, G., Price, M., Waterhouse, J.: Framework: assessing water in slope stability. In: Beale, G., Read, J. (eds.) Guidelines for Evaluating Water in Pit Slope Stability, pp. 19–64. CSIRO Publishing, Collingwood (2013)
12. Sánchez, E., Widzyk-Capehart, E., Poulson, J., Ortuño, F., Fredes, O., Steffen, S.: Slope stability management: coupling deformation measurements with pore pressure data using novel Networked smart markers platform. Water Min. (2016)
13. WIKA: Transductor de presión OEM. Available at: http://www.wika.cl/ti_1_es_es.WIKA. Accessed on 1 Sept 2015
14. Mikkelsen, P.E., Green, G.E.: Piezometers in fully grouted boreholes. In: Myrvoll (ed.) Field Measurements in Geomechanics, pp. 545–553. Lisse: Swets & Amp; Zeitlinger (2003)
15. Contreras, I.A., Grosser, A.T., VerStrate, R.H.: The use of the fully-grouted method for piezometer installation. Geotech. News **26**, 30–37 (2008)
16. ASTM D5084.: Standard Test Methods for Measurement of Hydraulic Conductivity of Saturated Porous Materials Using a Flexible Wall Permeameter. American Standard Testing Materials
17. NCh. 1515 of. 1979.: Determinación de la Humedad. Instituto Nacional de Normalización INN (1979)
18. NCh. 1532 of. 1980.: Densidad de Partículas Sólidas. Instituto Nacional de Normalización INN (1980)